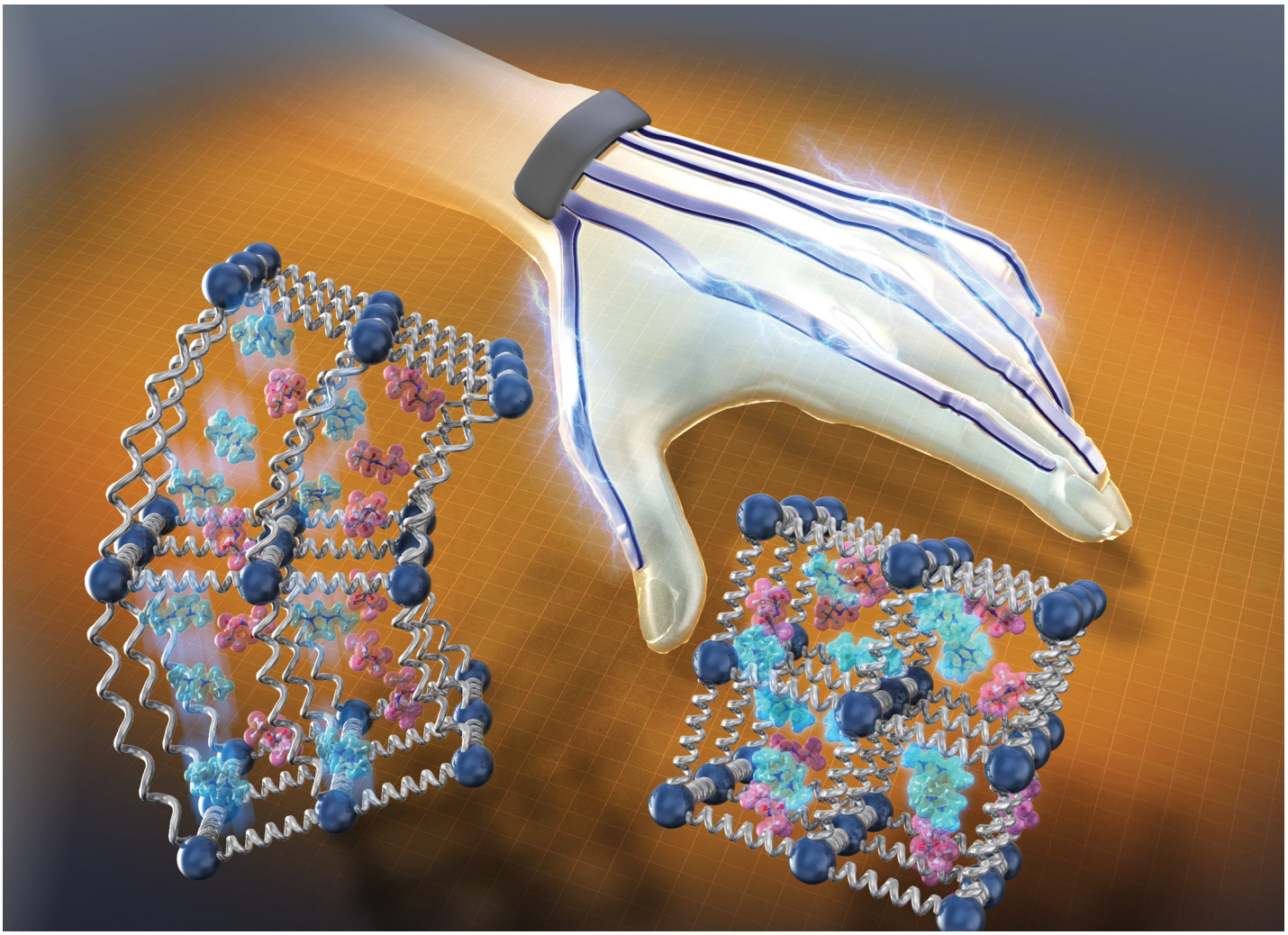

Highlighting research from the Conductive Polymer Laboratory led by Prof. Hidenori Okuzaki at the University of Yamanashi.

Ionic shape memory polymer gels as multifunctional sensors

A novel self-powered wearable sensor was fabricated using an ionic shape memory polymer (SMP) gel and the shape memory effect and sensor performance were investigated. It was found that the ionic SMP gel had potential as a wearable shape memory multifunctional sensor capable of generating electric charge and voltage in response to bending velocity and displacement, respectively.

As featured in:

See Hidenori Okuzaki *et al.*, *Soft Matter*, 2022, **18**, 6791.

ROYAL SOCIETY OF CHEMISTRY

rsc.li/soft-matter-journal

Registered charity number: 207890

Soft Matter

PAPER

View Article Online
View Journal | View Issue

Cite this: *Soft Matter*, 2022, **18**, 6791

Ionic shape memory polymer gels as multifunctional sensors†

YingJun An, Haruki Yoshida, Yuxin Jing, Tian Liang and Hidenori Okuzaki *

Received 23rd April 2022,
Accepted 12th August 2022

DOI: 10.1039/d2sm00515h

rsc.li/soft-matter-journal

Novel ionic shape memory polymer (SMP) gels were fabricated using SMPs and ionic liquids (ILs) of 1-ethyl-3-methylimidazolium bis(trifluoromethylsulfonyl)imide (EMI-TFSI) at different weight ratios (W_{IL}). The shape memory effect and sensor performance of the ionic SMP gels were investigated by means of thermomechanical and mechanoelectrical analyses. It was found that the ionic SMP gel at W_{IL} = 25 wt% showed a shape memory effect with the shape fixing ratio (R_f) and shape recovery ratio (R_r) of 72.7% and 72.9%, respectively. Upon bending, the ionic SMP gel sensors with PEDOT:PSS electrodes generated an open circuit voltage of 3.3 mV and a charge of 1.6 nC which linearly increased with increasing bending displacement and velocity, respectively. Furthermore, the wearable shape memory multifunctional sensor array was demonstrated as a self-powered motion sensor for IoT applications.

1 Introduction

The 'Internet of Things (IoT)' is a system that connects between people and things and between things through the Internet, such as health monitoring using heart rate sensors, remote control of home appliances using wearable devices, and gait measurement using sole sensors.[1–3] Herein, low-cost, lightweight, and flexible organic electronics[4,5] are a key technology for the IoT applications such as wearable sensors. In general, traditional wearable sensors can be divided into two types. One is piezoresistive sensors that detect changes in resistance of conductors such as graphenes,[6] carbon nanotubes (CNTs),[7] conductive polymers,[8] and metal nanowires[9] under stretching or bending. However, high power consumption, in which electric current always flows through the conductors, is a technical issue for the practical use.[10] The other is piezocapacitive sensors that detect changes in capacitance of dielectrics such as polydimethylsiloxane (PDMS)[11] and polyurethane under compression measured with an amplifier, but difficult to recognize the deformation direction, which is not suitable for motion sensors. In the era of IoT, we will live surrounded by a huge number of sensors, so-called 'trillion sensors', where power supply to all sensors and amplifiers is a serious problem. Therefore, self-powered sensors such as poly(vinylidene fluoride) (PVDF)[12,13] are typical ferroelectric polymers with a large dipole moment and have been intensively studied as flexible piezoelectric sensors generating voltages by bending deformation. Moreover, triboelectric sensors,[14,15] capable of transforming applied mechanical force into electricity, have been paid considerable attention as an energy harvesting and self-powered sensor. However, the output of both piezoelectric and triboelectric sensors is spike-like voltage signals in response to the mechanical deformation, which are hard to detect slow human motions and steady states as human–machine interfaces.

On the other hand, ionic polymers are also available as self-powered sensors.[16] Asaka and coworkers reported on ionic polymer–metal composite (IPMC) sensors using a Nafion film plated with gold electrodes, in which a voltage of less than 1 mV was generated by bending.[17] Kamamichi *et al.*[18] found that a bucky gel cantilever generated a voltage of *ca.* 0.1 mV even under a large bending displacement. The mechanism of ionic polymer sensors can be explained in terms of the 'piezoionic effect'[19] where polarization due to the movement of ions induced by deformation is responsible for generating the voltage. Although the ionic polymer sensors are self-powered systems without power supplies and amplifiers, the generated voltages are quite low (<1 mV), limiting their applications to the IoT. In this study, a novel self-powered wearable sensor was fabricated using an ionic shape memory polymer (SMP) gel and investigated the shape memory effect and sensor performance. It was found that the ionic SMP gel had the potential as a wearable shape memory multifunctional sensor capable of generating a voltage as high as 3.3 mV.

2 Experimental section

2.1 Materials

The polyurethane-based shape memory polymer (SMP, MM-6520) with a nominal glass transition temperature (T_g) of 65 °C

Graduate Faculty of Interdisciplinary Research, University of Yamanashi, 4-4-37 Takeda, Kofu, 400-8510, Japan. E-mail: okuzaki@yamanashi.ac.jp

† Electronic supplementary information (ESI) available. See DOI: https://doi.org/10.1039/d2sm00515h

was purchased from SMP Technologies Inc.[20] The ionic liquid (IL) of 1-ethyl-3-methylimidazolium bis(trifluoromethylsulfonyl)imide (EMI-TFSI) was purchased from Kanto Chemical Industry and used as received. The PEDOT:PSS water dispersion with a solid content of *ca.* 2.4 wt% used as electrodes was synthesized in our laboratory by oxidative polymerization of EDOT (Aldrich) monomers in the presence of PSS (M_w = 75 000 g mol^{-1}) as previously reported.[21,22] Ethylene glycol (EG, Kanto Chemical) as a secondary dopant to improve the electrical conductivity of the PEDOT:PSS,[23,24] ammonia solution (1M, Kanto Chemical) as a neutralizer, and *N*,*N*-dimethylacetamide (DMAc, Kanto Chemical) were used as received.

2.2 Fabrication

The SMP was dissolved in DMAc at a concentration of 10 wt% and mixed with the IL of EMI-TFSI at different weight ratios (W_{IL}). After vigorous stirring, the mixtures were drop cast and dried at Teflon dishes for 2 days at 50 °C, then dried at 200 °C under an N_2 atmosphere for 2 hours to remove the solvent completely. The ionic SMP gel film with a thickness of *ca.* 300 μm was peeled off from the Teflon dish, and the PEDOT:PSS water dispersion containing 10 wt% of EG was spin-coated at 500 rpm for 60 s on both sides of the ionic SMP gel and subsequently heated at 120 °C for 30 min with a moisture analyzer (MOC-120H, Shimadzu) not only to control temperature precisely, but also to monitor weight loss during heating.

2.3 Measurements

The FT-IR spectra of SMP, EMI-TFSI, and ionic SMP gel were measured by the attenuated total reflection (ATR) method using an infrared spectrophotometer (FT/IR-4200, Jasco). The dynamic mechanical analysis (DMA) of the ionic SMP gels (5 mm long, 2 mm wide, and *ca.* 300 μm thick) was carried out using TMA/SS6200 (Hitachi High-Tech) under a constant tension measured at a heating rate of 2 °C min^{-1} and a frequency of 0.1 Hz. The thermomechanical analysis (TMA) was performed with TMA/SS6200 (Hitachi High-Tech) using a tensile fixture at a force control mode. The SEM and element mapping images of the ionic SMP gel sensor were measured using an electron probe micro analyzer (EPMA, JXA-iHP200F, JEOL) at an accelerating voltage of 10 kV. The mechanoelectrical response of the ionic SMP gel sensors (15 mm long, 5 mm wide, and *ca.* 300 μm thick) was evaluated by measuring the generated voltage and charge with a data logger (NR-500, Keyence) and charge amplifier (NR-CA04, Keyence) under bending deformation induced with a mechanical tester (EZ-TEST, Shimadzu) at various displacements (d = 3, 5, and 7 mm) and velocities (v = 0.8, 1.7, and 3.3 mm s^{-1}).

3 Results and discussion

3.1 Structure and thermomechanical properties

Fig. 1(a) illustrates an ionic SMP gel composed of EMI-TFSI as ionic liquids (ILs) and SMPs, in which the EMI-TFSI is highly miscible with the SMP and produces a uniform and transparent gel at IL contents (W_{IL}) up to 25 wt%. A further increase of the W_{IL}, however, brought about a leakage of the IL from the gel, indicating the maximum uptake of the IL in SMPs was *ca.* 25 wt%. Fig. 1(b) shows the FT-IR spectra of SMPs, EMI-TFSI, and ionic SMP gels (W_{IL} = 25 wt%), indicating that the SMP is a typical polyether-based polyurethane with absorptions at 1707 cm^{-1} (C═O), 1066 cm^{-1} (C–O), 3311 cm^{-1}, 1533 cm^{-1} (N–H), and 1108 cm^{-1} (C–O–C).[25] Furthermore, the absorptions at 1599 cm^{-1} (C═C), 1223 cm^{-1}, 829 cm^{-1}, and 759 cm^{-1} (C–H) can be assigned to 4,4′-diphenylmethane diisocyanate (MDI).[25] Thus, the plausible chemical structure of SMPs inferred from FT-IR and previous patents[26,27] is shown in Fig. S1 (ESI†), where hard segments, composed of MDI and reactants of bisphenol A and ethylene oxide, connected to soft segments of polypropylene glycol. On the other hand, absorptions at 1350 cm^{-1} (S═O), 1190 cm^{-1} (C–F), and 1055 cm^{-1} (S–N) belong to the $TFSI^-$ of ionic liquids. It is noted that the ionic SMP gel (W_{IL} = 25 wt%) shows both absorption peaks of SMP and EMI-TSFI, indicative of their mixture without specific reactions.

The viscoelastic properties of the ionic SMP gels were evaluated by dynamic mechanical analysis (DMA), and the results are shown in Fig. 2. It was found that the SMP (W_{IL} = 0 wt%) showed a steep drop of storage modulus (E') and large loss tangent ($\tan\delta$) peak at 63 °C, corresponding to the glass transition temperature (T_g), where soft segments in the reversible phase of the segmented polyurethane block copolymer transfer from glass to rubber state while phase separated hard segments form hard domains by physical crosslinks through hydrogen bonding.[20] Notably, an increase of the W_{IL} significantly decreases both storage modulus at 20 °C ($E'_{20\,°C}$) and T_g, demonstrating that the IL in the ionic SMP gel acts as a plasticizer[28] that enhances the micro-Brownian motion of polymer chains. To develop wearable sensors with both shape memory and piezoionic effects available near body temperature (36 °C), the ionic SMP gel at W_{IL} = 25 wt% (T_g = 22 °C) was used for further investigation.

Fig. 3(a) shows a thermally induced shape memory effect consisting of two processes: One is the programming process where the ionic SMP gel heated above T_g is deformed by an external force (strain changes from ε_0 to ε_1) and then cooled down below T_g to fix the temporary shape (strain relaxes from ε_1 to ε_2). The other is the recovery process where heating of the ionic SMP gel with the temporary shape above the T_g will release the stored stress, which results in a recovery of the ionic SMP gel from the temporary to its original shape (strain recovers from ε_2 to ε_3).[20] The thermomechanical analysis (TMA) curves of the SMP (W_{IL} = 0 wt%) (Fig. 3(b)) and ionic SMP gel (W_{IL} = 25 wt%) (Fig. 3(c)) were measured for evaluating the shape memory effect. The specimen (5 mm long, 2 mm wide, and *ca.* 300 μm thick) was first heated to 70 °C above T_g at a heating rate of 5 °C min^{-1} and stretched under a constant stress of 0.5 MPa, then cooled down to *ca.* 10 °C to fix the shape with a temporary strain of ε_1. After releasing the stress, the sample slightly relaxed with a fixed strain of ε_2. Finally, the sample recovered from its temporary shape to the original shape with a recovery strain of ε_3 by heating again from room temperature to 70 °C. The shape fixing ratio (R_f) and shape recovery ratio (R_r) were, respectively, calculated as follows:

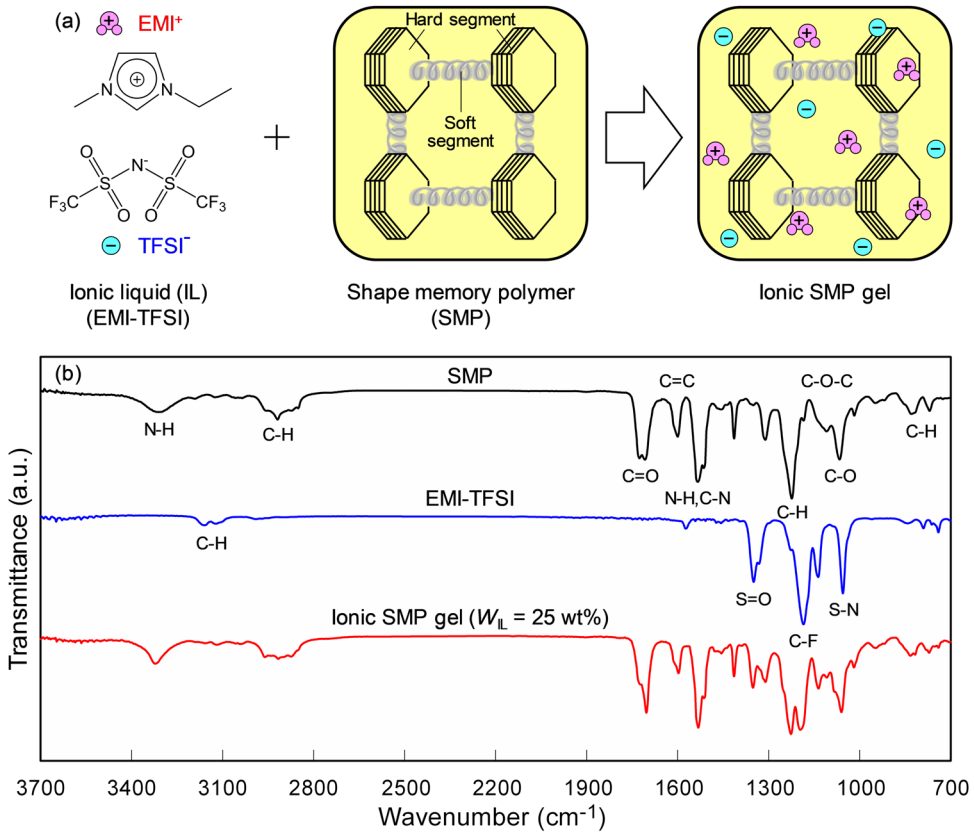

Fig. 1 (a) Schematic illustration of ionic shape memory polymer (SMP) gel composed of ionic liquids (EMI-TFSI) and SMPs. (b) FT-IR spectra of SMPs, EMI-TFSI, and ionic SMP gels (W_{IL} = 25 wt%).

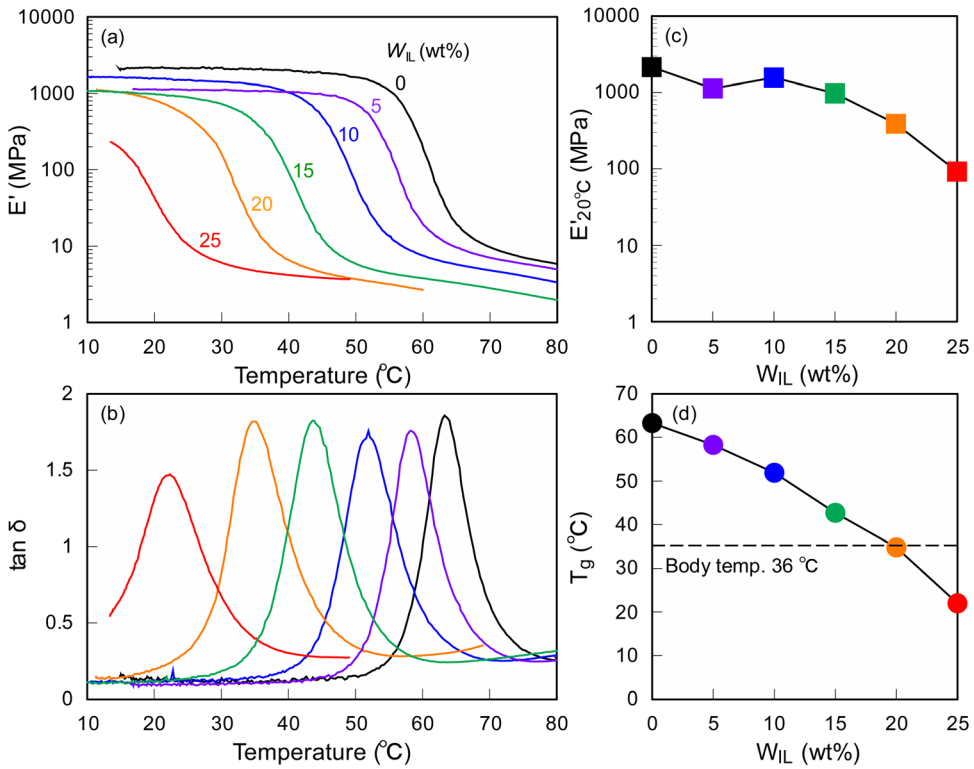

Fig. 2 Temperature dependence of (a) storage modulus (E') and (b) loss tangent (tan δ) for ionic SMP gels with different W_{IL}. Dependence of (c) storage modulus at 20 °C ($E'_{20\,°C}$) and (d) T_g of ionic SMP gels on W_{IL}.

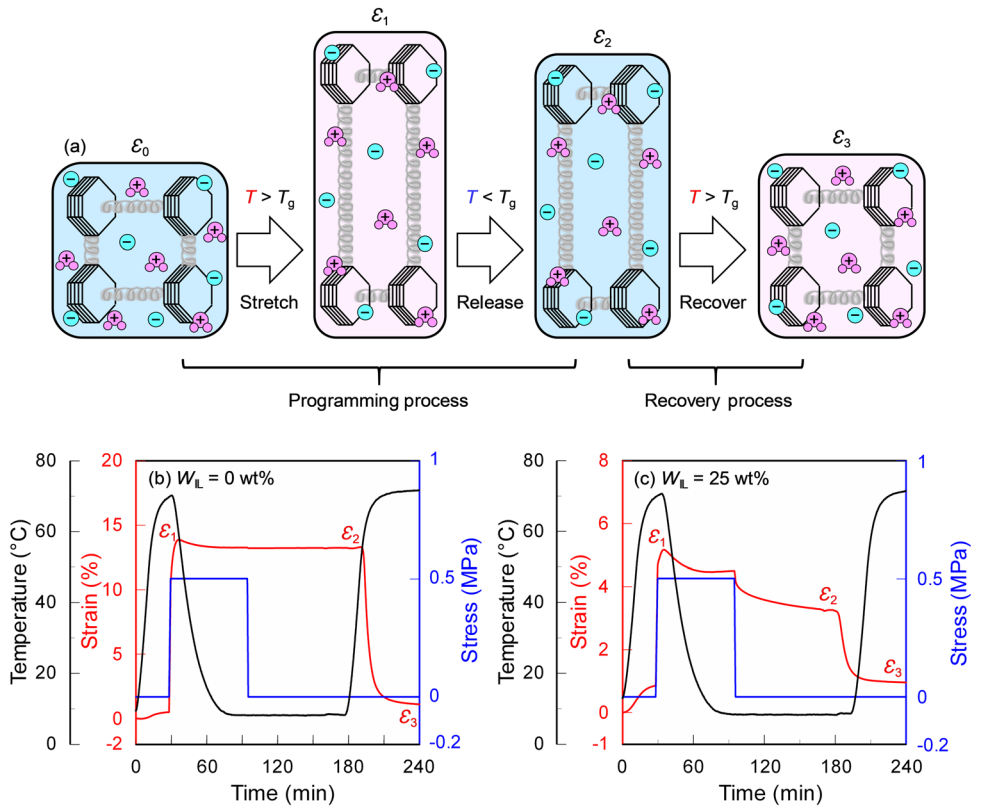

Fig. 3 (a) Schematic diagram of the shape memory effect of an ionic SMP gel. TMA curves of (b) SMPs (W_{IL} = 0 wt%) and (c) ionic SMP gels (W_{IL} = 25 wt%) where temperature (on the left of the plot), strain, and stress curves correspond to black, red, and blue lines, respectively. The specimen (5 mm long, 2 mm wide, and *ca.* 300 μm thick) was first heated to 70 °C above T_g at a heating rate of 5 °C min^{-1} and stretched under a constant stress of 0.5 MPa, then cooled down to *ca.* 10 °C to fix the shape with a temporary strain of ε_1. After releasing the stress, the sample slightly relaxed with a fixed strain of ε_2. Finally, the ample recovered from its temporary shape to the original shape with a recovery strain of ε_3 by heating again from room temperature to 70 °C.

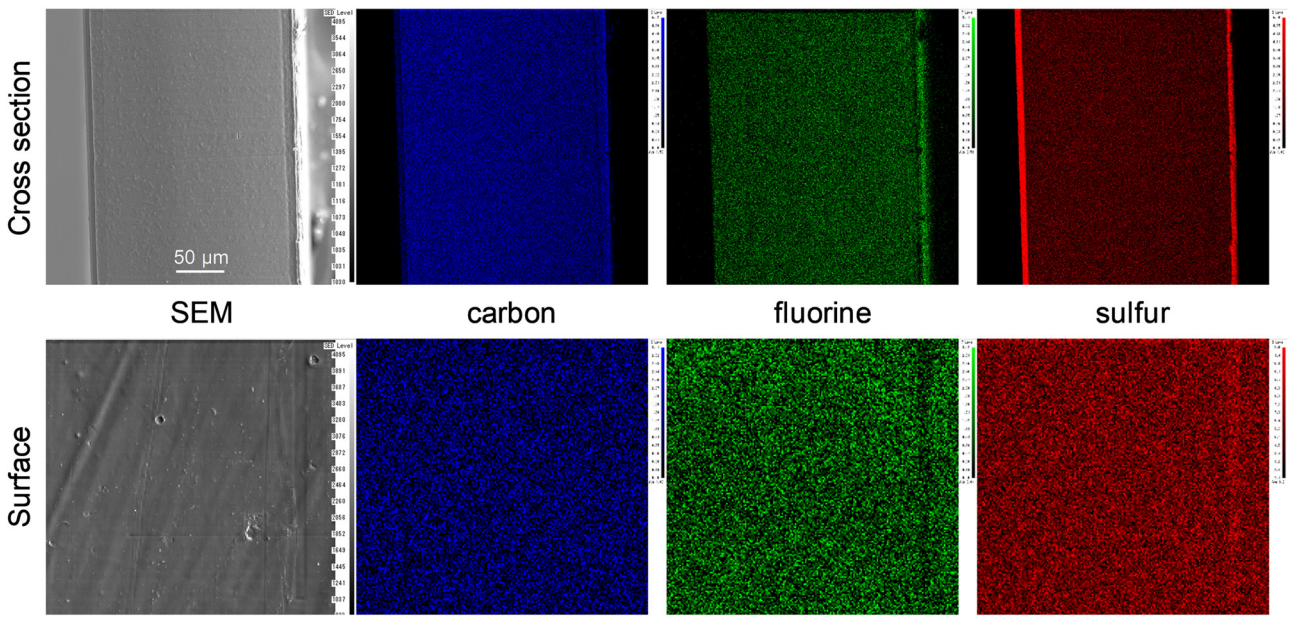

Fig. 4 SEM and EPMA element mapping images (blue: carbon, green: fluorine, and red: sulfur) of cross section and surface of the ionic SMP gel sensor with PEDOT:PSS electrodes on both surfaces of the gel (W_{IL} = 25 wt%).

$$R_f\,(\%) = (\varepsilon_2/\varepsilon_1) \times 100$$

$$R_r\,(\%) = (\varepsilon_2 - \varepsilon_3)/\varepsilon_2 \times 100$$

It is found that the SMP (W_{IL} = 0 wt%) exhibits excellent performance (R_f = 99.9% and R_r = 93.2%), whereas the ionic SMP gel (W_{IL} = 25 wt%) still keeps the shape memory effect with the R_f and R_r values of 72.7% and 72.9%, respectively. This can be ascribed to the plasticizing effect of EMI-TFSI, where a decrease of E' and T_g values of the SMP (Fig. 2) lowers both forces to keep the temporary shape and to recover its original shape, leading to the decrease of R_f and R_r values.

3.2 Multifunctional sensors

Fig. 4 shows SEM and EPMA element mapping images of the ionic SMP gel sensor with PEDOT:PSS electrodes on both surfaces of the gel (W_{IL} = 25 wt%). The distribution of carbon in the cross section (blue) clearly shows the sample in the SEM image, where fluorine (green) originated from $TFSI^-$ distributed homogeneously in the ionic SMP gel due to the high miscibility between SMPs and ionic liquids achieved by the solution casting method. Herein, the higher sulfur density at both surfaces can be explained by the PEDOT:PSS electrodes fabricated by spin coating. The SEM and EMPA element mapping images of the surface also support the homogeneous distribution of elements and smooth surfaces (except for a few small holes) without phase separation and aggregation at the microscopic level. It is noted that fluorine is observed on the surface because the detectable depth of EPMA (*ca.* 1 μm) is larger than the thickness of the PEDOT:PSS electrode (*ca.* 100 nm). Compared to other electrodes such as carbon nanotubes/ionic liquid composites and chemically plated gold or platinum,[16–18] the PEDOT:PSS is more flexible capable of fabricating by a facile wet-process such as spin-coating, bar-coating, dip-coating, and even spray-coating.[28,29]

As shown in Fig. 5(a), the ionic SMP gel sensor (15 mm long, 5 mm wide, and *ca.* 300 μm thick) was placed on a home-build sample holder, in which 5 mm at one end of the sensor strip was clamped with two gold electrodes to allow independent electrical contact with the PEDOT:PSS electrodes. The other end of the sensor strip was bent with the mechanical tester (Fig. 5(b)) at different bending displacements (d = 3, 5, and 7 mm) and velocities (v = 0.8, 1.7, and 3.3 mm s^{-1}) at a constant temperature of 36 °C. Fig. 6 shows the relation between input mechanical stimuli of constant bending displacement (d = 7 mm) (a) with different velocities (v = 0.8, 1.7, and 3.3 mm s^{-1}) (b) and output electric signals of voltage (V) (c) and electric charge (q) (d) of ionic SMP gel sensors (W_{IL} = 25 wt%). Upon bending, a large positive q was generated, followed by a small negative q, while the opposite phenomenon was observed when the bent film recovers to the original straight shape. Here, the generation of charge is associated with the movement of EMI^+ and $TFSI^-$ ions in the gel induced by the bending deformation, suggesting that the EMI^+ can move faster than $TFSI^-$. In general, the transference number of ions strongly depends not only on the size but also on the shape and charge distribution of ions. Indeed, the EMI^+ ions have higher transference number (t_+ = 0.63) than $TFSI^-$ ions (t_- = 0.37) evaluated by NMR measurements.[30] We should emphasize that the ionic SMP gel sensor generated a voltage (V) of 3.3 mV which is an order of magnitude larger than conventional ionic polymer–metal composite (IPMC) sensors.[17] To evaluate the reliability of sensing, the bending cycle was repeated 10 000 times. It was found that no notable change and hysteresis in both electric charge (Fig. S2, ESI†) and voltage (Fig. S3, ESI†) demonstrating high stability and reproducibility of the ionic SMP gel sensor. For the practical use, the ionic SMP gel sensor can be laminated with polymer films to keep away from moisture which will affect the piezoionic effect.[17] It is noted here the strong correlations between d and V and between v and q indicate multifunctional sensors, capable of transducing different input mechanical stimuli into corresponding output electric signals. Further investigation was carried out at constant v = 3.3 mm s^{-1} with different d = 3, 5, and 7 mm, and the results are shown in Fig. 7. One can see that the input mechanical stimuli correspond well with the output electric signals similarly to Fig. 6, where V (c) and q (d) are generated independently in response to d (a) and v (b), respectively.

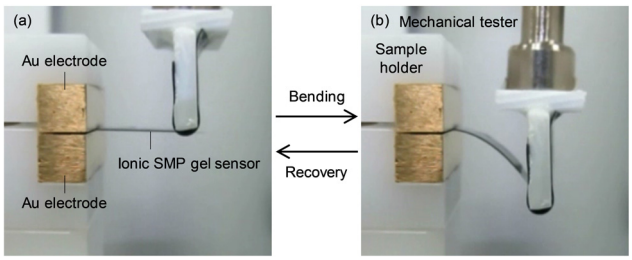

Fig. 5 (a) Experimental setup for evaluating ionic SMP gel sensors with PEDOT:PSS electrodes on both surfaces of the gel (W_{IL} = 25 wt%) where 5 mm at the left end of the sensor (15 mm long, 5 mm wide, and *ca.* 300 μm thick), placed on a PET sheet (100 μm thick) used as the substrate, was clamped with gold electrodes. (b) The ionic SMP gel sensor was bent by pushing down the right end with a mechanical tester at different bending displacements (d = 3, 5, and 7 mm) and velocities (v = 0.8, 1.7, and 3.3 mm s^{-1}) at a constant temperature of 36 °C.

A clear indication of the importance of an ionic SMP gel as a multifunctional sensor is demonstrated in Fig. 8(a and b). It was found that the values of V and q increase linearly with increasing d and v, where sensitivities corresponding to each slope of the straight lines obtained by fitting with the least-squares method were 0.37 V m^{-1} and 0.47 μC s m^{-1}, respectively. Different from the conventional piezoelectric phenomenon, the mechanism of ionic SMP gel sensors can be explained in terms of the 'piezoionic effect' as depicted in Fig. 8(c).[19,31] In the initial state of the ionic SMP gel sensor, both EMI^+ and $TFSI^-$ ions distribute homogenously in the gel. Upon bending, the dissociated EMI^+ and $TFSI^-$ ions would migrate from the compressed side to the expanded side because of the concentration gradient in the curved ionic SMP gel. In fact, the strain difference on both sides of the gel ($\Delta\varepsilon$) was calculated using the free length (L = 10 mm), thickness (t = *ca.* 300 μm), and bending displacement (d) as follows:[28,29]

$$\Delta\varepsilon\,(\%) = 2td/(L^2 + d^2) \times 100$$

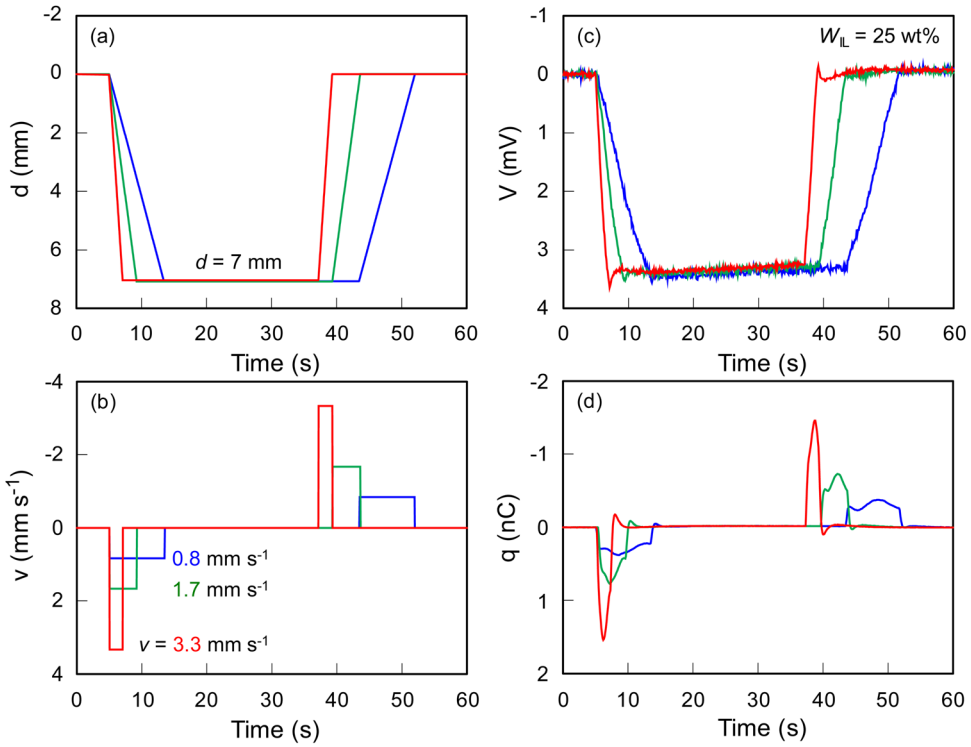

Fig. 6 Relation between input mechanical stimuli of (a) constant bending displacement (d = 7 mm) with (b) different velocities (v = 0.8, 1.7, and 3.3 mm s^{-1}) and output electric signals of (c) voltage (V) and (d) electric charge (q) of ionic SMP gel sensor (W_{IL} = 25 wt%).

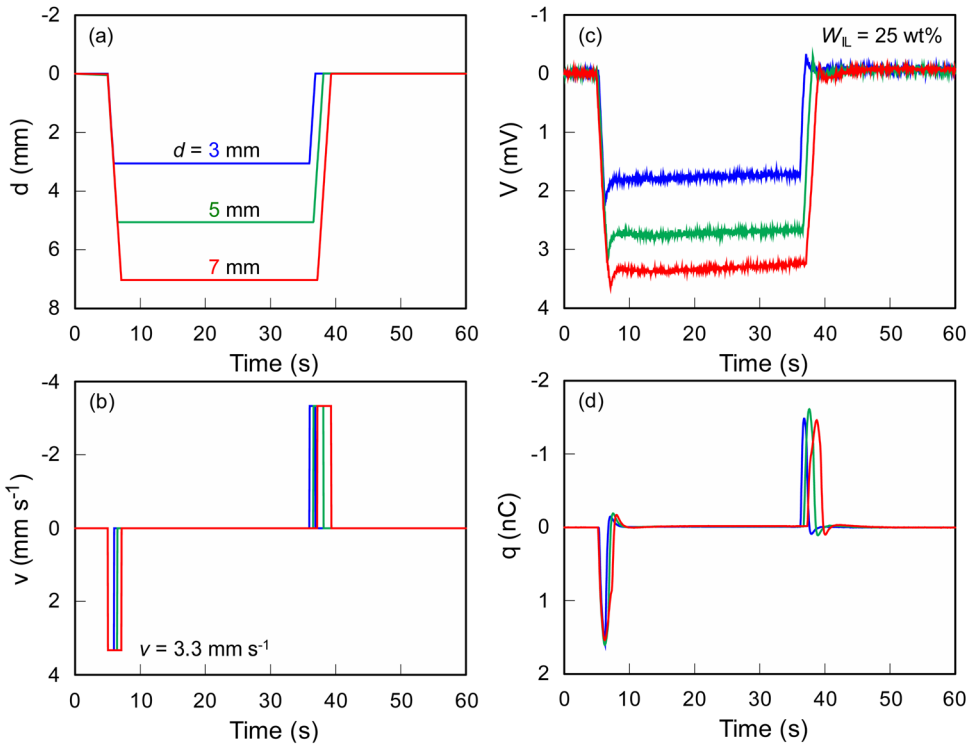

Fig. 7 Relation between input mechanical stimuli of (a) constant bending velocity (v = 3.3 mm s^{-1}) with (b) different displacements (d = 3, 5, 7 mm) and output electric signals of (c) voltage (V) and (d) electric charge (q) of ionic SMP gel sensor (W_{IL} = 25 wt%).

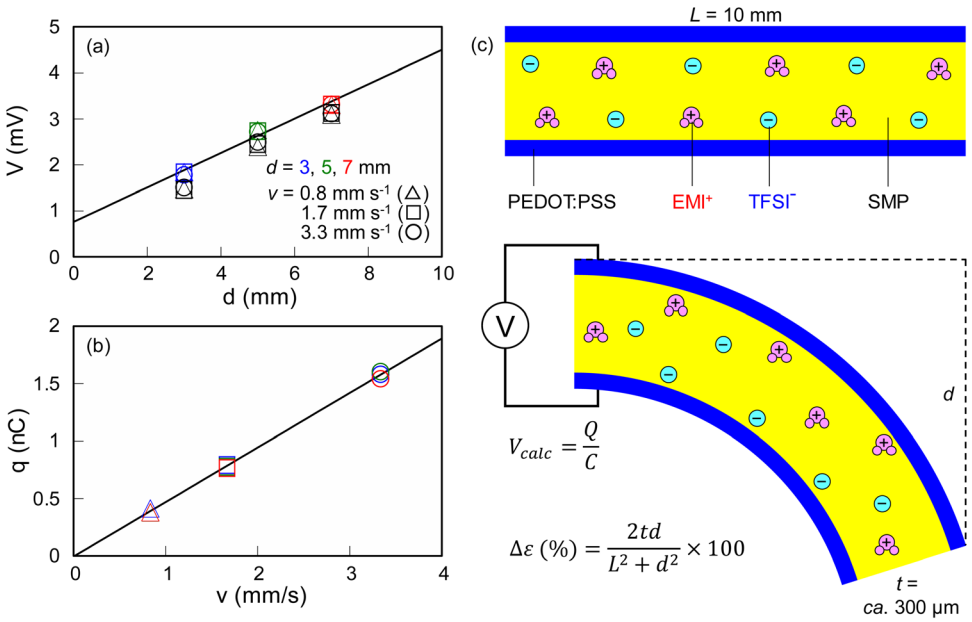

Fig. 8 Relation (a) between V and d and (b) between q and v of ionic SMP gel sensor (W_{IL} = 25 wt%) measured at d = 3 (blue), 5 (green), 7 mm (red) and v = 0.8 (Δ), 1.7 (□), 3.3 mm s^{-1} (○) with calculated voltages (V_{calc}) defined as $V_{calc} = Q/C$ represented by black symbols where straight lines were obtained by fitting with the least-squares method. (c) Schematic illustration of a possible mechanism of piezoionic effect in ionic SMP gel sensor.

Although the range of d seems to be narrow, the bending at d = 7 mm is quite large (Fig. 5b) where the value of $\Delta\varepsilon$ tends to level off at $d > 7$ mm (Fig. S4, ESI†). Since the EMI^+ ions have a higher transference number than $TFSI^-$ ions,[30] bending the ionic SMP gel sensor causes the EMI^+ ions to move rapidly toward the expanded outer surface, producing the positive q, followed by $TFSI^-$ ions producing the negative q. To clarify the detailed mechanism of the piezoionic effect more quantitively, the actual transference numbers in the SMP gel can be evaluated by the solid-state NMR technique.[30] Furthermore, the mechanism of voltage generation can be explained using the overall net positive charge (Q_+) and net negative charge (Q_-) calculated as shown in Fig. S5 (ESI†), where q is the charge generated at the moment but Q_+ and Q_- represent the total amount of electric charges. If the Q_+ value is not in balance with the Q_- value due to the specific interactions between ionic liquids and polymer networks, the total amount charge ($Q = Q_+ + Q_-$) is stored in the ionic SMP gel under bending deformation, which will be the origin of the voltage generation. Indeed, the calculated voltages (V_{calc}) can be derived from the values of Q as follows:

$$V_{calc} = Q/C$$

where C is the capacitance of the ionic SMP gel (1.28 mF) determined using a current–voltage curve measured by an electrochemical impedance system (Fig. S6, ESI†). We should emphasize here that the values of V_{calc}, represented by the black open symbols in Fig. 8(a), are consistent with the measured V values regardless of the input mechanical stimuli such as d and v. This clearly shows that the piezoionic sensors can be represented by a simple capacitor expressed as $V = Q/C$. Therefore, there are two ways to enhance the output voltage of the piezoionic sensors: one is to increase the Q value where the large difference in transference numbers between cations (t_+) and anions (t_-) and the large strain difference on both sides of the gel ($\Delta\varepsilon$) are crucially important. The other is to reduce the C value where low W_{IL} and dielectric constant of the ionic gel are preferred. In addition, to improve sensor performance, the interaction between the IL and the polymer matrix should be clarified, affecting both Q and C values. The results suggest that the $TFSI^-$ ions may interact with the SMP matrices through ion-dipole interactions, resulting in the generation of large positive charges mainly by migration of EMI^+ in the gel. Furthermore, the sensor performance is dependent on the ionic liquid content (W_{IL}), where the ionic SMP gel sensor with $W_{IL} <$ 25 wt% showed a small response of both q and V probably due to the higher T_g than body temperature. Therefore, the systematic research to clarify the effect of W_{IL} and measurement conditions (temperature, humidity, *etc.*) on sensor performance is currently underway. Moreover, since the role of PEDOT:PSS electrodes with a negative zeta potential (−50 mV) in water[32] on sensor performance is still unclear, the detailed mechanism can be clarified in future work where Kelvin probe force microscopy is available to observe the local charge state.

3.3 Application to wearable sensors

Based on the piezoionic phenomenon of the ionic SMP gel, we have devised wearable shape memory multifunctional sensors. Fig. 9(a) shows the shape memory effect of the ionic SMP gel sensor, in which the temporary flat shape recovers to the initial curved shape on a finger because the body temperature (*ca.* 36 °C) is higher than T_g of the ionic SMP gel (22 °C). This indicates that the ionic SMP gel sensor can fit on a variety of curved surfaces, allowing us to develop an on-demand wearable sensor by adapting to individual body shapes. Furthermore, a

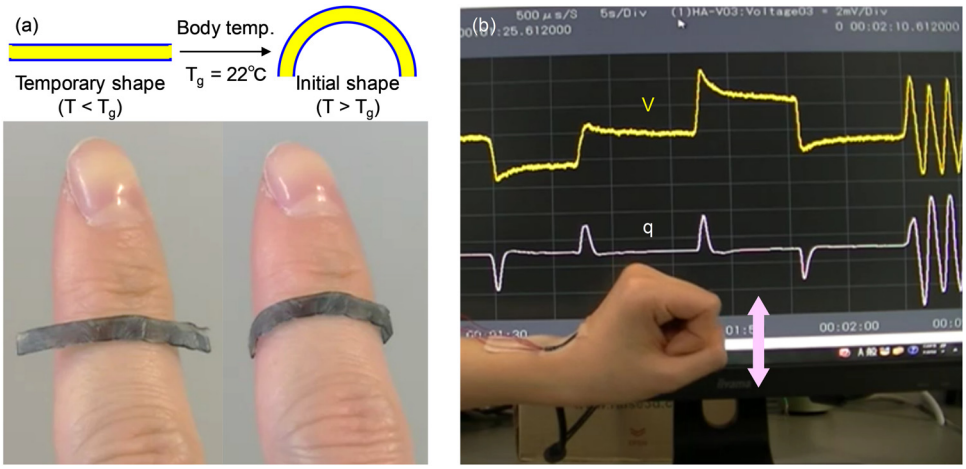

Fig. 9 (a) Schematic and photographs of ionic SMP gel sensor (W_{IL} = 25 wt%) with shape memory effect where temporary flat shape ($T < T_g$) recovers to initial curved shape on a finger at body temperature ($T > T_g$). (b) Photograph of a wearable sensor, fabricated with two equivalent ionic SMP gel sensors arranged in parallel by lamination with polyester films (100 μm thick), attached to the wrist detecting voltage (V) and charge (q) in response to shaking the wrist up and down.

sensor array with two equivalent ionic SMP gel sensors arranged in parallel was fabricated by lamination with polyester films (100 μm thick) to detect the different mechanical stimuli at the same time. As revealed in Fig. 9(b), the sensor array attached to the wrist generates positive and negative voltages and charges in response to shaking the wrist up and down, indicative of the multifunctional sensors capable of sensing both direction and quantity of bending displacement and velocity. Unlike the power-consuming piezoresistive sensors, the piezoionic sensor using the ionic SMP gel is a self-powered displacement sensor without a power supply and amplifier, which may open up a new field of wearable multifunctional motion sensors such as virtual reality, healthcare, and robots for the IoT applications. Furthermore, the non-power flexible sensors using ionic SMPs can be applied to power generators and electric double-layer capacitors for energy harvesting.

4 Conclusion

The ionic SMP gels composed of EMI-TFSI and SMPs were fabricated at different W_{IL}. The increase of W_{IL} significantly decreased the T_g of the ionic SMP gel due to the plasticizing effect. It was found that the ionic SMP gel at W_{IL} = 25 wt% with T_g = 22 °C exhibited the shape memory effect of R_f = 72.7% and R_r = 72.9%. The values of V and q, generated by bending the ionic SMP gel sensor increased in proportion to the d and v with the sensitivities of 0.37 V m^{-1} and 0.47 μCs m^{-1}, respectively. The results allowed us to conclude that the ionic SMP gel sensors could be applied to self-powered wearable shape memory multifunctional sensors in a wide field of IoT applications.

Author contributions

YingJun An: design, methodology, measurements, data curation, and draft writing; Haruki Yoshida: measurements, data analysis, demonstration, and draft editing; Yuxin Jing: data analysis, demonstration, and draft editing; Tian Liang: methodology, measurements, and data curation; Hidenori Okuzaki: supervision, conceptualization, fund acquisition, project management, draft review and editing.

Conflicts of interest

There are no conflicts of interest to declare.

Acknowledgements

This work was supported by JSPS KAKENHI Grant Number JP20K05616 of Grant-in-Aid for Scientific Research(C).

References

1 K. Ashton, That ‘‘internet of things’’ thing, *RFID J.*, 2009, **22**, 97–114.
2 P. A. Laplante, M. Kassab, N. L. Laplante and J. M. Voas, Building caring healthcare systems in the internet of things, *IEEE Syst. J.*, 2018, **12**, 3030–3037.
3 R. S. Raji, Smart networks for control, *IEEE Spectrum*, 1994, **31**, 49–55.
4 H. Klauk, *Organic Electronics: Materials, Manufacturing and Applications*, Wiley-VCH, Weinheim, 2006.
5 H. Klauk, *Organic electronics II: More Materials and Applications*, Wiley-VCH, Weinheim, 2010.
6 C. Yan, J. Wang, W. Kang, M. Cui, X. Wang, C. Y. Foo, K. J. Chee and P. S. Lee, Highly stretchable piezoresistive graphene-nanocellulose nanopaper for strain sensors, *Adv. Mater.*, 2014, **26**, 2022–2027.
7 T. Yamada, Y. Hayamizu, Y. Yamamoto, Y. Yomogida, A. Izadi-Najafabadi, D. N. Futaba and K. Hata, A stretchable

carbon nanotube strain sensor for human-motion detection, *Nat. Nanotechnol.*, 2011, **6**, 296–301.

8 M. Z. Seyedin, J. M. Razal, P. C. Innis and G. G. Wallace, Strain-responsive polyurethane/PEDOT:PSS elastomeric composite fibers with high electrical conductivity, *Adv. Funct. Mater.*, 2014, **24**, 2957–2966.

9 C. Pang, G.-Y. Lee, T.-I. Kim, S. M. Kim, H. N. Kim, S.-H. Ahn and K.-Y. Suh, A flexible and highly sensitive strain-gauge sensor using reversible interlocking of nanofibres, *Nat. Mater.*, 2012, **11**, 795–801.

10 Y. H. Jung, S. K. Hong, H. S. Wang, J. H. Han, T. X. Pham, H. Park, J. Kim, S. Kang, C. D. Yoo and K. J. Lee, Flexible piezoelectric acoustic sensors and machine learning for speech processing, *Adv. Mater.*, 2020, **32**, 1904020.

11 S. Y. Kim, S. Park, H. W. Park, D. H. Park, Y. Jeong and D. H. Kim, Highly sensitive and multimodal all-carbon skin sensors capable of simultaneously detecting tactile and biological stimuli, *Adv. Funct. Mater.*, 2015, **27**, 4178–4185.

12 H. Kawai, The piezoelectricity of poly(vinylidene fluoride), *Jpn. J. Appl. Phys.*, 1969, **8**, 975.

13 L. Persano, C. Dagdeviren, Y. Su, Y. Zhang, S. Girardo, D. Pisignano, Y. Huang and J. A. Rogers, High performance piezoelectric devices based on aligned arrays of nanofibers of poly(vinylidenefluoride-*co*-trifluoroethylene), *Nat. Commun.*, 2013, **4**, 1633.

14 F. Fan, Z. Tian and Z. Wang, Flexible triboelectric generator, *Nano Energy*, 2012, **1**, 328–334.

15 R. Liu, X. Kuang, J. Deng, Y.-C. Wang, A. C. Wang, W. Ding, Y.-C. Lai, J. Chen, P. Wang, Z. Lin, H. J. Qi, B. Sun and Z. L. Wang, Shape memory polymers for body motion energy harvesting and self-powered mechanosensing, *Adv. Mater.*, 2018, **30**, 1705195.

16 M. Shahinpoor and K. J. Kim, Ionic polymer-metal composites: I. Fundamentals, *Smart Mater. Struct.*, 2001, **10**, 819–833.

17 Z. Zhu, T. Horiuchi, K. Takagi, J. Takeda, L. Chang and K. Asaka, Effects of cation on electrical responses of ionic polymer-metal composite sensors at various ambient humidities, *J. Appl. Phys.*, 2016, **120**, 084906.

18 N. Kamamichi, M. Yamakita, K. Asaka, Z.-W. Luo and T. Mukai, Sensor property of a novel EAP device with ionic-liquid-based bucky gel, *IEEE Sensors*, 2007, **28-31**, 221–224.

19 V. Woehling, G. T. M. Nguyen, C. Plesse, Y. Petel, Y. Dobashi, J. D. W. Madden, C. A. Michal and F. Vidal, Study of the piezoionic effect and influence of electrolyte in conducting polymer based soft strain sensors, *Multifunct. Mater.*, 2019, **2**, 045002.

20 Y. An and H. Okuzaki, Novel electro-active shape memory polymers for soft actuators, *Jpn. J. Appl. Phys.*, 2020, **59**, 061002.

21 T. Horii, H. Hikawa, M. Katsunuma and H. Okuzaki, Synthesis of highly conductive PEDOT:PSS and correlation with hierarchical structure, *Polymer*, 2018, **140**, 33–38.

22 Y. Kurushima, N. Katsuyama and H. Okuzaki, Effect of PEDOT:PSS composition on photovoltaic performance of PEDOT:PSS/n-Si hybrid solar cells, *Jpn. J. Appl. Phys.*, 2021, **60**, 091001.

23 M. Yamashita, C. Otani, M. Shimizu and H. Okuzaki, Effect of solvent on carrier transport in poly(3,4-ethylenedioxythiophene)/poly(4-styrenesulfonate) studied by terahertz and infrared-ultraviolet spectroscopy, *Appl. Phys. Lett.*, 2011, **99**, 143307.

24 T. Takano, H. Masunaga, A. Fujiwara, H. Okuzaki and T. Sasaki, PEDOT nanocrystal in highly conductive PEDOT:PSS polymer films, *Macromolecules*, 2012, **45**, 3859–3865.

25 E. Fujimoto and K. Nakamura, Analysis of photodegradation mechanism of polyurethane using FT-IT-ATR and DMA, *Kobunshi Ronbunshu*, 1994, **51**, 612–618.

26 S. Hayashi and H. Fujimura, *Shape memory polymer form*, *US Pat.*, 1991, 5049591.

27 S. Hayashi, *Shape memory polyurethane elastomer molded articles*, *US Pat.*, 1992, 5145935.

28 Y. Li, R. Tanigawa and H. Okuzaki, Soft and flexible PEDOT/PSS films for applications to soft actuators, *Smart Mater. Struct.*, 2014, **23**, 074010.

29 H. Okuzaki, S. Takagi, F. Hishiki and R. Tanigawa, Ionic liquid/polyurethane/PEDOT:PSS composites for electroactive polymer actuators, *Sens. Actuators, B*, 2014, **194**, 59–63.

30 S. Imaizumi, Y. Kato, H. Kokubo and M. Watanabe, Driving mechanisms of ionic polymer actuators having electric double layer capacitor structures, *J. Phys. Chem. B*, 2012, **116**, 5080–5089.

31 Y. Liu, Y. Hu, J. Zhao, G. Wu, X. Tao and W. Chen, Self-powered piezoionic strain sensor toward the monitoring of human activities, *Small*, 2016, **12**, 5074–5080.

32 T. Wakabayashi, M. Katsunuma, K. Kudo and H. Okuzaki, pH-Tunable high performance PEDOT:PSS aluminum solid electrolytic capacitors, *ACS Appl. Energy Mater.*, 2018, **1**, 2157–2163.